Observation of molten pool movement during laser welding

Ing. Petr Vondrouš

Vedoucí práce: prof. Ing. Jiří Dunovský, CSc., prof. Seiji Katayama

Abstrakt - CZE

Příspěvek se zabývá pozorováním proudění taveniny při keyhole laserovém svařování pomocí RTG záření a výzkum byl experimentálně proveden v Laboratoři laserového svařování profesora Katayama na Univerzitě Osaka. Rentgenové záření prochází svařovaným vzorkem a je snímáno vysokorychlostní kamerou. Pozorování toku taveniny odhaluje výrazně odlišné chování material a napomáhá osvětlit vznik vad svaru jako porosity, rozstřiku, solidifikačních trhlin atd. Jsou využity 2 různé materiály, litina s kuličkovým grafitem a nízkolegovaná Cr-Mo ocel. Chování taveniny těchto dvou materiálů je porovnáno a materiály mají výrazně odlišné proudění taveniny z hlediska rychlosti a směru proudění.

Klíčová slova

Laser, LBW, svařování, tok taveniny, RTG, LKG, nízkolegovaná ocel

Abstract - ENG

The research observes molten metal flows during keyhole laser welding using X-ray transmission system. Research was done at Katayama Laser Welding Laboratory at Osaka University. X-ray is transmitting through welded sample and recorded by high speed camera. Melt flows observation clarifies creation of welding defects as porosity, spatter, solidification cracks. Two materials, ductile iron and Cr-Mo low alloy steel are observed and their melt flows are mapped. The flows are significantly different in speeds and directions.

Keywords

Laser, LBW, welding, melt flow, X-ray, ductile iron, low alloy steel

1. Introduction

Laser beam welding (LBW) is a fusion welding technology, which is based on heating up 2 pieces of material (usually metals) over the melting temperature. These molten materials mix up in created molten pool and upon cooling they solidify to create weld. It is obvious that creation of molten pool and its behavior are crucial for weld formation. Molten pool behavior can be understood as melt volume, melt movement (direction, speed), melt mixing etc. This molten pool behavior influences heat and mass transfer in the weld, influences size and shape of weld (WM and HAZ), mixing of metals, solidification rate, segregation etc. It was also found that molten pool movements influence creation of weld defects, e.g. entrapped porosity, creation of solidification cracks.

As an example of importance of molten pool behavior, well know example of GMAW welding of steel can be shown. Weld penetration reached by GMAW welding of steel in active gas atmosphere (presence of O_2, CO_2 in inert gas) is higher than when welded in pure inert atmosphere. This is caused because of Marangoni flow (temperature gradient surface tension driven flow) of molten metal is altered by oxygen presence. Oxygen presence causes changes in molten pool movement direction from outward (in presence of inert atmosphere) to outward (in presence of oxygen), resulting in deepening of weld penetration [1].

Laser welding is modern fusion welding technology that receives a lot of attention from the industry (automotive, aviation, electronics), because it is very promising technology because of its weld precision, quality, speed and efficiency. Specifics of laser beam (energy density, light as heat source) welding make the process different from standard arc welding processes and the molten pool behavior is not yet well understood in LBW. To elucidate phenomena of molten pool behavior two often used materials were observed during LBW. X-ray transmission in-situ imaging system was used to observe molten metal flows inside the weld molten pool. All experiments were conducted at the Laser Welding Laboratory of professor Katayama at Osaka University during author`s stay there. Processing of results was done at home university, Czech Technical University in Prague.

2. Experimental setup

Ductile iron and low alloy Cr-Mo steel are materials often used in automotive industry for construction of engine, powertrain components, e.g. gear and shaft, gear and gear case. These two materials can be considered as basic examples of engine parts that are prospectively suitable for LBW. These materials are subjected to research of molten pool movement during bead-on-plate (further BOP) welding.

2.1 Used materials

Used materials are ductile iron FCD600 and low alloyed steel SCM420. It is considered that this selection represents irons (high carbon content iron materials) and steels (low carbon content materials) in general, so approximately these results would be valid for wide spectra of materials.

Both selected materials, FCD600, SCM420, are using denomination according to japanese JIS norms, because research was conducted in Japan. Their respective international equivalents are also stated.

FCD600 is ductile iron (C 3.4 %, Si 2.5 %, other). It has pearlitic-feritic matrix with nodular graphite. The material has high tensile strength, good castability enabled by low melting point (1150°C), high melt fluidity, and is often used for castings of pistons, valves, tubes, gears. Equivalent of this material is DIN GGG60.

SCM420 is high strength low alloy Cr-Mo steel (C 0.2 %, Cr 1.1 %, Mo 0.15 %, Mn 0.8 %, other). Material has melting temperature around 1530°C, solidification interval of about 40°C. The matrix is pearlitic-feritic. Material is suitable for heat treatment, has high tensile, fatigue strengths and is used for gears, shafts, pistons and other engine components that need surface treatment, e.g. case hardening . The closest material equivalent is DIN 25CrMo4 and SAE 4130.

2.2 Laser source, welding head

Modern fiber laser by company IPG with maximum power 10 kW was used. Laser source properties are in Tab. 1.

Tab. 1 Laser source parameters

Manufacturer	IPG
Maximum power	10 kW
Wavelength	1070 nm
BPP	12 mm*rad
Fiber core diameter	0.3 mm
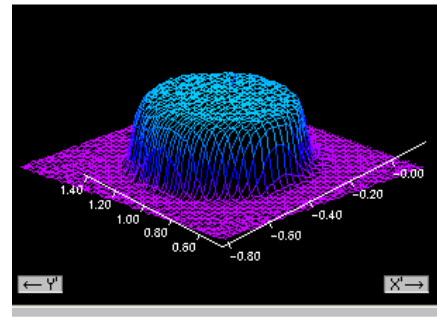
Fig. 1.: Fiber laser beam tophat profile

As welding head Precitec welding head with collimation lense f=125 mm and focusing lens f=250 mm was used, giving theoretical spot diameter 0.6 mm. From measurement of the beam profile by laser quality measurement unit Primus, tophat beam profile of diameter 0.572 mm was measured. Beam profile as measured in laser beam focus is show at the Fig. 1.
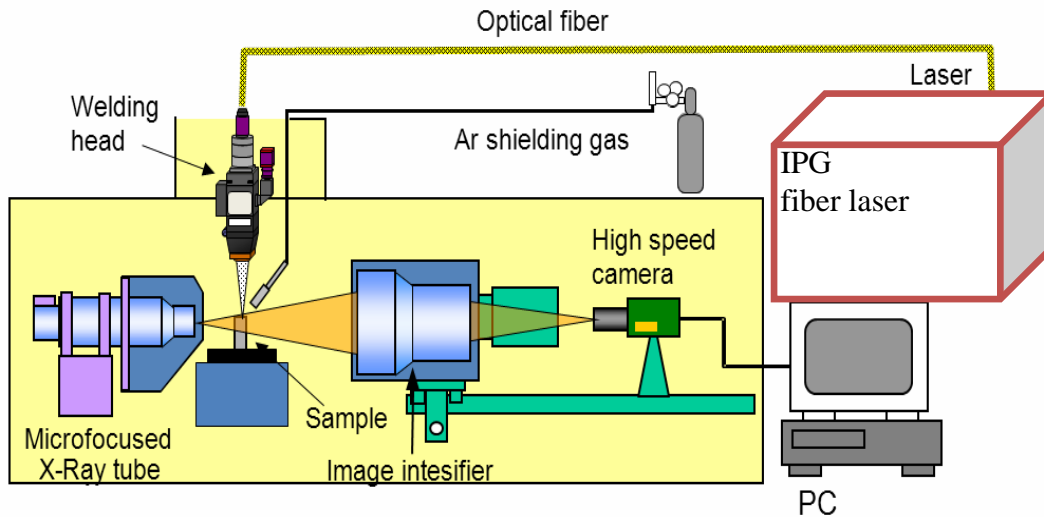

Fig. 2.: Welding setup of laser and X-ray device

2.3 Welding setup of laser and X-ray

Laser is connected to welding head by optical fiber of 0.3 mm diameter. Thin sample is mounted onto moving stage that executes the movement. Perpendicularly to the sample X-ray system coupled with high speed video camera is used to observe the inner metal flow inside the molten pool and keyhole stability. As shielding gas argon is used. The welding setup is shown at the Fig. 2.

2.4 Sample preparation, W particle inserts

Thin sample of dimensions 150x30x6 mm is used for X-ray observation. The original sample of 150x40x30 mm needed to be thinned down to thickness 6 mm, because of limited power of X-ray tube. Into the sample the small holes were drilled and small globular W particles were inserted, holes were filled with wire afterwards. Insertion of W particles with high density enables observance of molten metal flow by X-ray device. Sample is shown on Fig. 3.
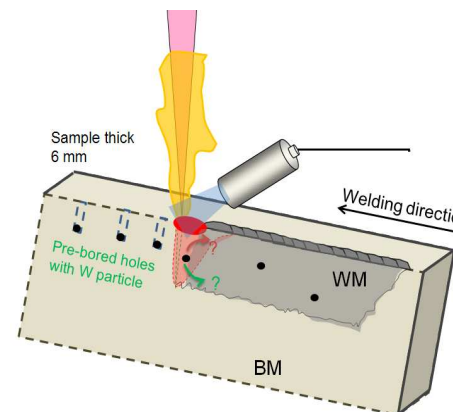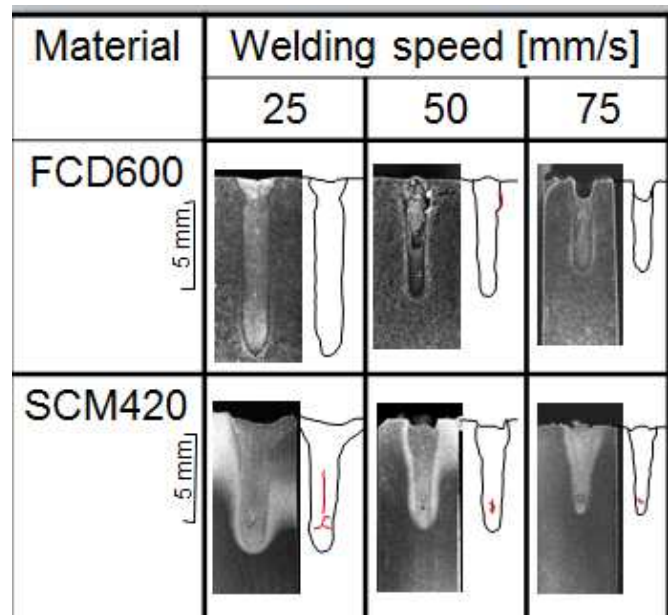

Fig. 3.: Sample with W particles

2.5 Experiment and weld evaluation

The optical metallography was the main method to assess welds` shape and weld quality. Molten metal flow was observed by analysis of high speed video cameras data, where W particles movement trajectories were observed together with keyhole stability. Speed of W particles and dominant trajectories were drawn, diameters and stability of keyhole were compared for both materials.

3. BOP Welding results

Bead on plate (BOP) welding with variation of welding speed, 25, 50, 75 mm/s, with constant continuous laser power 8 kW were done. This means heat input per unit length was 320, 160, 80 J/mm. Welds were shielded by Argon gas with flow of 30 l/min. Focal point was at the upper surface of the specimen. Their metallography cross sections are shown at Fig. 4, on the right side of the macrographs are schematics showing weld shape in black color and welding defects in red.


Fig. 4 Cross sections of examined welds

Both materials have deep and quite narrow welds, with high weld shape ratio (weld depth/ weld width). There is obvious difference between the two materials, where the penetration, weld shape and occurring defects differ significantly with the material.

At the Fig. 5 we can see graphs of weld depth, width and weld area for both materials. Weld area is approximately the same for all welding speeds, but the width and depth differ significantly. Weld shape ratio (depth to width) varies 4-5.5 for FCD600 and 2.5-4 for SCM420.

From the fact that weld area for both materials is almost the same, we can expect that heat input into the weld (for the same welding speed) is same. This means that laser beam energy coupling into the metal is also almost the same and the reason for the difference of weld depth and width between the materials is be caused by difference in molten metal flow. The research of molten metal flow is justified and necessary.
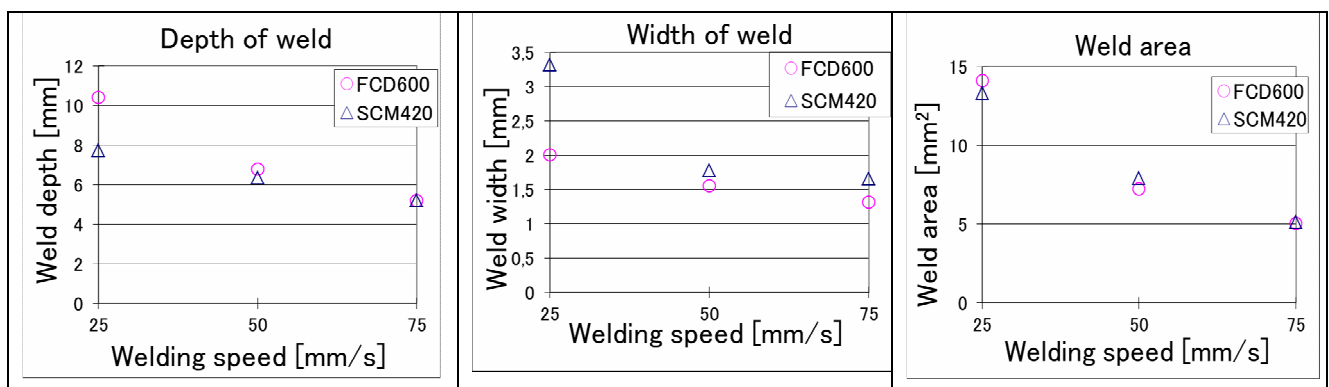
Fig. 5 Graphs of weld depth, weld widths and weld area for iron FCD600 and steel SCM420

At Fig. 4 various welding defects are visible for both metals. Visible are cracks, spatter and subsequent underfill, undercut and porosity. Most serious defects are solidification cracks found in SCM420. The severity of spatter, undercut, underfill and porosity is increasing with welding speed.

Even though not visible at Fig. 4 and not observed at samples prepared for X-ray observation, in majority of welds` in ductile iron FCD600 the welding cracks have been observed. These could be described as vertical and perpendicular cracks in WM and HAZ. Also weld bead perpendicular cracks were present in majority of the weld beads with FCD600. It was found that the welding heat cycle is causing brittle cementite creation. With heating up graphite nodules partially dissolve into austenite matrix and upon fast cooling the cementite structure are formed. In such a brittle structure cracks easily form. It needs to be stated that in thin samples for X-ray observation these cementite brittle cracks were greatly suppressed, because of low rigidity of the welded specimen, which is very thin.

4 Melt flow observation

After observing the melt flows for each material separately for all the welding speeds 25, 50, 75 mm/s, same flow patterns were undoubtedly visible. Because of these similarities, it was decided to evaluate X-ray results on sample welded with 25 mm/s, because this welding speed creates the deepest keyhole and widest and deepest molten pool, where the movement is most easily observable.
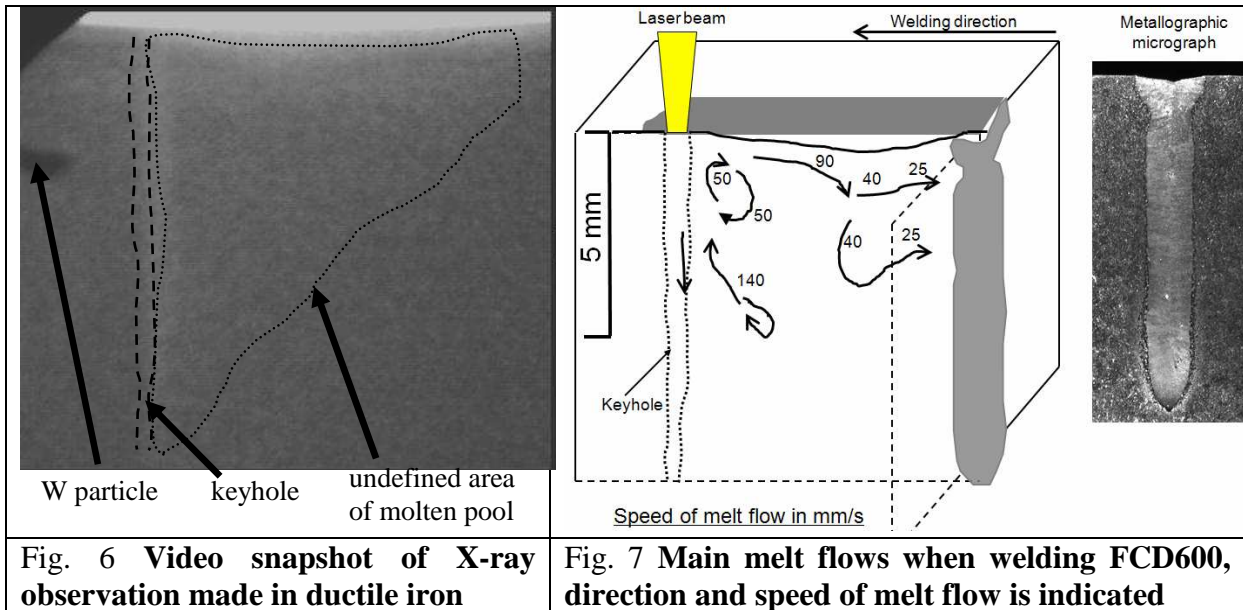
4.1 Melt flow in FCD600 (ductile iron), 25 mm/s, 8 kW

Very deep keyhole is created by incident laser beam in the ductile iron. The dimensions of the keyhole were measured and are shown in Tab. 2. Keyhole depth 10.7. mm with average diameter of 0.5 mm. The keyhole has conical shape, with maximum diameter at the top and minimum diameter at the bottom, this conical shape is in concordance with literature [1]. Shape of the keyhole is caused mainly by force balance of vapor recoil pressure and surface tension. It can be noted that upper keyhole diameter (0.65 mm) is very close to beam spot diameter (0.6 mm). Sufficiently deep and wide keyhole is clue showing good laser beam energy absorption. Keyhole pulsations were clear in the video. Sometimes the keyhole collapsed and porosity was formed behind.

Tab. 2 Keyhole depth and width

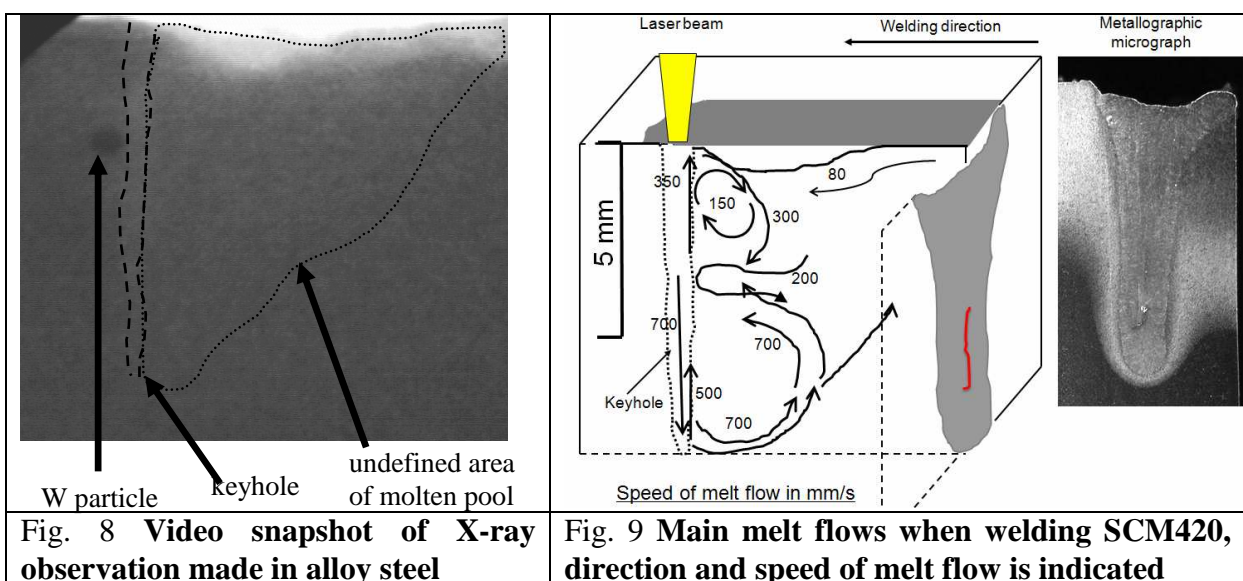| Material		FCD600 ductile iron	SCM420 low alloy steel
Keyhole depth [mm]		10.7	7.7
Keyhole diameter [mm]	At the top	0.65	0.95
	In the middle	0.5	0.6
	At the bottom	0.3	0.35
	Average	0.5	0.65

As an example of data obtained from X-ray transmission observation is shown at Fig 6. After completing observation of the X-ray video main result of melt flows is shown at Fig. 7. Fast downward flow existed inside the keyhole and was caused by the recoil pressure of a laser beam. Directly behind the keyhole there was an upward flow of 140 mm/s. Slow circular flow with the speed of around 50 mm/s existed in the upper area behind the beam. This circular flow might cause "wine cup" widening visible at the very top part of the metallographic micrograph. With an increase in the distance from the keyhole the speeds of melt metal flows decreased. It is concluded that the melt metal flows for FCD600 were rather simple and slow with a speed range of 25 – 140 mm/s.

| Fig. 6 **Video snapshot of X-ray observation made in ductile iron** | Fig. 7 **Main melt flows when welding FCD600, direction and speed of melt flow is indicated** |

4.2 Melt flow in SCM420 (Cr-Mo low alloy steel), 25 mm/s, 8 kW

Dimensions of keyhole created in SCM420 are shown in Tab. 2. The keyhole depth is 7.7 mm, average diameter 0.65 mm. Compared to FCD600 it not so deep, but has much higher diameter.

The observation results of melt flows are shown in Fig. 9. A fast downward flow existed inside the keyhole, reaching up to 700 mm/s. This is probably results of laser beam radiation pressure influencing the fall of W particle in vapor filled keyhole cavity. Fast upward flows of 350 -500 mm/s were observed closely behind the keyhole and at the keyhole wall. Upward flow is caused by interaction of ejected plume and melt due to viscosity. Circular clockwise flow existed at a speed of 150 mm/s in the upper area behind the laser beam. These flows are causing certain widening of the weld at the weld upper part. There was a very fast anti clockwise circular flow (700 mm/s) in the lower half of the weld. Further behind the keyhole there existed flows inwards to the keyhole. Melt metal flows observed in SCM420 were complex in the speed ranges of 80 - 700 mm/s.

| Fig. 8 **Video snapshot of X-ray observation made in alloy steel** | Fig. 9 **Main melt flows when welding SCM420, direction and speed of melt flow is indicated** |

4.2.1 Fractography analysis of solidification cracks

By fractography analysis it was found out that fracture occurring in SCM420, are solidification cracks. Cracks were observed to be only in WM, often at the bottom. When fractured surface was observed under high magnification in scanning electron microscope (SEM), dendritic surface was visible. Furthermore sulphur inclusions were diagnosed by spectroscopic analysis XDS.

When fact that cracks occurring in SCM420 are solidification cracks is put together with data of melt flows, it is obvious that reason for crack formation are fast melt flows occurring in SCM420. Especially strong and fast melt flow at the bottom of the weld, at Fig. 9 circular movement of speed 500-700 mm/s, causes wide solidification mushy zone at the weld bottom. This causes significantly prolonged solidification of the melt in this area, and problems of segregation and shrinkage are aggravated here. Thus solidification crack can be easily created.

4.2.2 Suppression of the solidification cracks

Any research in technological area, if it encounters some real problem, should serve to find counter measures. For our case of creation of solidification cracks, the question how to suppress solidification cracks has arisen.

The solidification cracks are caused solidification stresses, when these are accompanied by unfavorable solidification process sequence and low material strength, e.g. caused by presence of impurities in WM. The sequence of solidification and thermal stresses distribution can be easily visible in weld shape. It is known and obvious that weld shape can be altered by defocused distance, laser beam angle etc. Thus experiments with defocused distance, full penetration welds, laser beam inclination were done.

During the experiments with defocused distance variation (variation of fd), it was found that high negative defocused distance causes weld with V shape, narrow at the bottom, wider at the top [2]. When weld has V shape, it then complies with an inscribed circle method, known from the foundry industry. Such a shape ensures unidirectional solidification from the weld bottom to the weld top and minimizes the shrinkage stresses. Also the segregation would be better distributed in the weld.

Other possibility are full penetration welds. Because partial penetration welds are subjected to higher weld contraction stresses, than full penetration welds, because of weld root opposing to weld shrinkage. No cracks have been found in the cross sections, so it can be stated, that full penetration weld is more resistant to solidification cracking and is more suitable than partial penetration welding as was proven. Inclination of the laser beam to suppress solidification cracks was not successful.

5. Discussion - Differences in behavior between 2 materials

As stated in chapter 3, 4 and in [2], many differences in behavior of ductile iron FCD600 and Cr-Mo steel SCM420 during laser welding under the same welding conditions have been found.

Main differences were observed in size of created keyhole, molten metal flows (speed, directions), plume behavior. These differences result in different penetration depth, weld shape, type of occurring cracks, spattering and so on. Mainly physical and chemical properties of both materials are considered to be the cause of these differences. One of differences is in fluidity, i.e. viscosity. In foundry literature is stated, that fluidity of iron increases with C, Si, P values and Cr alloying decreases fluidity [3, 4]. Even though concrete values of fluidity for ductile iron and Cr-Mo low alloy steel are not exactly known, in literature were found values of viscosity (reciprocal value of fluidity). Approximate viscosity for steel is equal 0.043E-

$5m^2/s$ and for ductile iron $0.030E-5m^2/s$. It is obvious that ductile iron FCD600 (because of C, Si content) has much better fluidity than SCM420.

Main forces governing keyhole and melt movements during keyhole mode laser welding are recoil pressure, surface tension, Marangoni flow (surface tension temperature dependence). [5, 6] Plume friction influence was not considered as important force, but in recent research its significance was experimentally proven [7]. Our results of X-ray observation for FCD600 and SCM420 suggest that plume melt friction influence is important. Lower viscosity of FCD600 enables deeper keyhole formation because of balance of forces in keyhole creation.

It is expected that reason for fast lower circular flow for SCM420 is connected mainly with keyhole instability. When keyhole collapses, vapor recoil pressure

Both materials have poor laser weldability because of crack formation. In ductile iron brittle cracks due to cementite formation occurs and in Cr Mo low alloy steel solidification cracks form. Possibility to suppress cracking of both alloys needs to be considered to solve weldability. Cracking of FCD600, where cracks due to Fe_3C are caused by thermal stresses and presence of brittle cementite, can be suppressed by lowering thermal stresses and (or) volume of brittle cementite. To reduce thermal stresses upon cooling preheat can be applied. During the BOP welding of FCD600 preheat up to 300 °C was done, but it had no possitive influence on suppressing the cracks. Probably preheat of up to 600 °C would have effect, but it was not possible to reach this high temperature in our experiments. To lower cementite volume, usage of ductile Ni wire for butt joint is feasible. Carbon is well soluble in Ni, so cementite presence is suppressed and WM hardness is lowered. This was successfully used for butt welding and welds using Ni filler were without cracks.

6. Conclusion

The ductile iron and low alloy Cr-Mo steel were subdued to BOP laser welding to research weld metal flows inside the molten pool by X-ray transmission observation system. It can be concluded, that both materials behavior greatly varies. Both materials laser weldability is poor, because cracks are occurring in both metals.

Laser beam is creating deeper and narrower keyhole in FCD600, which results in very deep welds, with high weld aspect ratio. Created keyhole is deep 10.7 mm, is unstable at the bottom and creation of spatter is easy and is causing underfill. Ease of spatter creation is caused by welding parameters (power density) and strong vapor plume. Melt flow is quite simple and rather slow, speed 25-140 mm/s. Low viscosity and therefore low forces of interaction plume melt are considered to be cause of limited and slow melt flow.

Keyhole created in SCM420 has higher diameter and lower depth, resulting in wider bead and lower penetration depth. Solidification cracks occur in this material under all welding conditions near the weld bottom and thermal axis. Solidification cracks are caused by complex fast metal flows that prolong solidifcation.

Melt flows show great difference. As difference in material properties influencing greatly melt flows is viscosity (fluidity) of both metals, which is in the core of plume melt friction interaction. Further research would be needed to approve or reject importance of this force on melt flow during laser welding.

Literature

[1] Dawes, C., Laser welding, Woodhead Publishing, 1992, p. 147

[2] Vondrous P., Katayama S., Kawahito Y., Laser Welding of Ductile Iron and Low Alloy Steel, Japanese Welding Society Preprints, autumn 2010, Tokyo

[3] ASM Handbook, Volume 15, Casting, 2010 ASM International

[4] Bugayev K. et al., Iron and Steel Production, Beekman Books, Incorporated, 1971

[5] Pang S. et al., J. Phys D: Appl. Phys., 44, 2011

[6] Lee J. et al., J. Phys D: Appl. Phys., 35, 2002

[7] Katayama S., Kawahito Y., Elucidation of phenomena in high power fiber laser welding, Proceedings SPIE, 2010